DOE/PC/92533--T1

RADIATIVE PROPERTIES OF CHAR, FLY-ASH, AND SOOT PARTICLES IN COAL FLAMES

M. P. MENGÜÇ
S. MANICKAVASAGAM, R. GOVINDAN, and S. GHOSAL

DEPARTMENT OF MECHANICAL ENGINEERING
UNIVERSITY OF KENTUCKY
LEXINGTON, KY 40506

Q-4Q-9C

TECHNICAL PROGRESS REPORT: SECOND YEAR

PERIOD: SEPTEMBER 15, 1993 – SEPTEMBER 15, 1994

No: DOE/PC/92533-9

(GRANT #DE-FG22-92PC92533)

submitted to

DEPARTMENT OF ENERGY,
PITTSBURGH ENERGY TECHNOLOGY CENTER,
PITTSBURGH, PENNSYLVANIA

Preface

This is the second year Technical Progress Report of the project titled "Radiative Properties of Char, Fly-Ash, Soot Particles in Coal Flames". The period covered is from September 15, 1993 to September 15, 1994. This project has been funded by the Department of Energy, Pittsburgh Energy Technology Center through a grant #DE-FG22-92PC92533.

In this report, we summarize the experimental and the theoretical approaches taken in this project.

During this period, Dr. Sivakumar Manickavasagam and Dr. Sarbajit Ghosal served as part-time Research Associates. Dr. Ghosal's efforts have been concentrated on the experimental studies, particularly on the Nd:YAG laser diagnostic system. Dr. Sivakumar has also involved with these efforts. Additionally, he has been responsible from modeling particulate optical and radiative properties.

A third student, Mr. Ramaswamy Govindan, has been working towards his MS degree on this project. His research focus is on developing an experimental system where the elements of the Mueller (scattering) matrix can be measured. Once this system is coupled with the theoretical results produced by the agglomerate model algorithms, we will be able to determine local concentration distributions of different particles in pulverized-coal flames. (The first part of this report is based on the preliminary version of Mr. Govindan's M.S. thesis.)

In addition to these individuals, two other students had varying degrees of impact on this project. Mr. Zeljko Ivezic, who is currently a Ph.D. student at Physics and Astronomy used the DDSCAT algorithm to develop simple, yet helpful rules about the dependent/independent scattering regimes of soot agglomerates. On the other hand, Mr. Stig Alsted, an undergraduate student in Mechanical Engineering used the I-DEAS package to develop fractal-shape agglomerates for soot particles. The structures drawn from his work helped us to visualize the agglomerates in three-dimensional space. Later, the coordinates of these structures were input to the AGGLOME code developed by Dr. Manickavasagam to calculate the Mueller matrix elements of different structures.

So far, we have presented one poster at the 25th International Symposium on Combustion, which was held at Irvine, California and submitted a paper to a journal. In addition to these, a paper is being prepared. They are listed below:

1: S. Ghosal, S. Manickavasagam, R. Govindan, and M. P. Mengüç, "Light Scattering Experiments for Simultaneous Determination of Soot and Char Volume Fractions in Coal-Fired Flames", Poster Presentation at the 25th International Symposium on Combustion, Irvine, CA, August 1994.

2: Z. Ivezic and M.P. Mengüç, "An Investigation of Dependent-Independent Scattering Regimes for Soot Particles Using the Discrete Dipole Approximation", submitted to the *International Journal of Heat and Mass Transfer*, 1994.

3: S. Manickavasagam and M.P. Mengüç, "Mueller Matrix Components of Fractal-Like Soot Agglomerates", to be submitted to *Applied Optics*, 1994.

Please note that recently we were granted an extension by the DOE until May 30, 1995 for the completion of this project.

Contents

List of Figures

1 INTRODUCTION

In large-scale coal-fired flames, radiative transfer is significant as a large portion of the energy generated during the char pyrolysis and soot oxidation is transferred to the surroundings by radiation (due to *emission*). The relatively cold gases and particles which are not burning yet are heated by this incoming energy (*absorption*), which may have originated not only from the immediate surroundings of the control volume of interest but the entire flame. It is obvious that if the emission and absorption of radiation in such a flame are not accounted for correctly, it is not possible to determine other underlying phenomena with accuracy, as the fundamental principle of conservation of energy would be violated.

In order to consider the effect of radiation heat transfer in coal-fired furnaces, we have to 1) model the radiative transfer equation to satisfy the conservation of radiant energy principle; 2) use the correct radiative properties of combustion gases and particles; 3) account for the interaction of radiation with the flow and energy equations.

The radiative properties for a participating medium of spherical particles can be expressed in terms of the spectral absorption, extinction, and scattering efficiencies and the phase function for a single particle, and can be calculated from the Lorenz-Mie theory (van de Hulst, 1981; Bohren and Huffman, 1983). For small size particles, the expressions are based on the Rayleigh limit of Lorenz-Mie theory, and are significantly simpler. The details are readily available in the literature (van de Hulst, 1981; Bohren and Huffman, 1983).

1.1 Specific Objectives

The main objective of this work is to measure the significant elements of the scattering (Mueller) matrix in a coal-laden diffusion flame in order to identify the structure of particles in such flames. A multi-wavelength laser based diagnostic system is to be developed to measure the angular distribution of scattered intensity by the flame, using different combinations of polarizers and retarders. The data collected will be reduced by employing different inverse radiation algorithms and particle/agglomerate property models.

2 THEORETICAL MODELS

When an electromagnetic wave or a photon interacts with a medium containing small particles, the radiative intensity may be changed by absorption and/or scattering. How much and into which direction a particle scatters an electromagnetic wave passing through its vicinity depends on particle's

1. shape,
2. complex index of refraction, $m = n - ik$

3. relative size with respect to the wavelength, as well as

4. the clearance between particles.

The information about the scattered energy can be used to determine the physical properties of particles if the signals collected can be interpreted carefully. In this work we are specifically concerned with the problem of performing light scattering measurements in flames to obtain more information about the shape and volume fraction distribution of the particles.

When light in some arbitrary polarization state is incident on a medium, the polarization state of the scattered or transmitted light can be related to the polarization state of the incident light by a 4×4 matrix. This matrix, which is called the *Mueller Matrix*, is a characteristic of the medium. It depends on wavelength and, in the case of light scattering, is a function of the scattering angle. It yields invaluable information about the physical properties of the scattering particulates. It is a necessary and major part of the complete optical description of a medium. This matrix is going to be determined experimentally for the coal-laden flames, and the results will be compared against the theoretical values determined for different size coal particles and fractal-like agglomerates.

2.1 Literature Survey

Most of the previous work similar in nature to the present study have been performed in the field of atmospheric optics measurements. The earliest known work was carried out by Pritchard and Elliott (1960). They designed a polar nephelometer to measure six elements of the Mueller matrix for fog and clear air. They used six independent combinations of polarizers and analyzers to make scattered intensity measurements and then used subtractive techniques to recover the Mueller matrix elements. This technique is very time consuming because the polarizer and analyzer have to be replaced for each combination. Also because of the large time involved, the accuracy of these measurements is questionable. Beardsley (1968) measured the Mueller matrices of sea water using several independent combinations of polarizers and analyzers. Because each of the sixteen elements requires a different combination of settings, this technique takes significant amount of time and yields less accurate results.

Holland and Gagne (1970) used a polar nephelometer similar to the one developed by Pritchard and Elliott to measure all elements of the Mueller matrix for polydisperse systems of irregular, randomly oriented particles. These results were compared to the matrix elements that were calculated for assemblies of spherical particles that fit the same particle size distribution function and have the same refractive index. For this they recorded intensity information for eighteen combinations of filters and subsequently took differences between

the recorded values to obtain the matrix elements. The disadvantage of this technique is that the values needed to obtain the elements appear as small differences between relatively large quantities. Hence small errors introduced by drift and instabilities are magnified.

Kemp (1969) developed a piezo-optical birefringence modulator. This instrument is based on the piezo-optic or photoelastic effect (stress-induced birefringence). An acoustic vibration is set up in a block of isotropic transparent material, such as glass or fused silica; this vibration is sustained by a transducer. The resulting birefringence can be used to produce a beam of alternately left and right circularly polarized light for circular dichroism measurements.

Hunt and Huffman (1973) used the piezo-optical birefringence modulator developed by Kemp (1969) to construct a polarization-modulated light scattering instrument. This instrument consists of a polarizer and a modulator before the scattering cell and an analyzer after the scattering cell. They used two combinations of the modulator and polarizer angles with respect to the scattering plane to obtain six elements of the Mueller matrix. Experimental results were reported for polystyrene latex spheres dispersed in water and sulfur sols and compared with the Mie theory calculations. Since this instrument uses only one modulator, it could measure only the combinations of matrix elements. Perry, Hunt and Huffman (1978) made measurements to determine all sixteen elements of the Mueller scattering matrix for two types of non-spherical particles.

Thompson (1978) designed a sophisticated instrument to measure all sixteen elements of the Mueller matrix. He used a four modulator photo-polarimeter which makes use of four electro-optic modulators and two polarizers. Boyer, Lamouroux and Prade (1979) designed a system which measures the Stokes parameters of light automatically over a wide range of wavelengths. This system uses two piezo-optic modulators.

Recently, Kuik, Stammes and Hovenier (1991) designed an experimental setup to measure six independent elements of the Mueller matrix. By using a single electro-optic Pockels cell modulator along with two polarizers and a quarter wave plate, they were able to obtain the desired elements from four separate measurements. They reported results for irregularly shaped particles.

On the theoretical side, Fry and Kattawar (1981) and Hovenier, Van de Hulst and Van der Mee (1986) developed relationships between elements of the Mueller matrix. A complete set of nine independent equations describing these relationships was found.

From the literature survey it is evident that no attempts have been made to measure the Mueller matrix for particles in flames. In this work we use an instrument similar to the one used by Kuik, Stammes and Hovenier (1991) and consider the fact that for randomly oriented particles, the Mueller matrix has only six elements. Even though our method uses subtractive techniques to obtain the six elements, the accuracy is not affected because the

elements to be recovered appear as significant differences between large quantities.

2.2 Stokes Vector

We may represent a beam of arbitrary polarization, including partially polarized light, by a column vector, the Stokes Vector, the four elements of which are the Stokes parameters. The Stokes parameters may be expressed equivalently in terms of quadratic functions of the electric fields as

$$I = < E_{\|}E_{\|}^{*} + E_{\perp}E_{\perp}^{*} > \quad (1)$$

$$Q = < E_{\|}E_{\|}^{*} - E_{\perp}E_{\perp}^{*} > \quad (2)$$

$$U = < E_{\|}E_{\perp}^{*} + E_{\perp}E_{\|}^{*} > \quad (3)$$

$$V = i < E_{\|}E_{\perp}^{*} - E_{\perp}E_{\|}^{*} > \quad (4)$$

The subscripts refer to the components of the electric field parallel ($\|$), and perpendicular ($\perp$) to the scattering plane which is defined by the direction of the incoming and scattered waves. The angular brackets refer to time averages and the asterisks ($*$) denote the complex conjugates.

Here I represents the total intensity, Q the difference between the horizontal and vertically polarized intensities, U the difference between the $+45°$ and $-45°$ polarized intensities, and V the difference between the right-handed and left-handed circularly polarized intensities.

2.3 Mueller Matrix

In general, the state of polarization of a beam is changed on interaction with an optical element (for example, a polarizer, retarder, reflector or scatterer). Thus it is possible to represent such optical elements by a 4×4 matrix (Mueller, 1948). The *Mueller Matrix* describes the relation between "incident" and "transmitted" Stokes vectors; where "incident" refers to the beam before the interaction with the optical element, and "transmitted" is after that. Then, we can write

$$S_t = AS_i \quad (5)$$

where S_i and S_t represent the incident and transmitted Stokes vectors, respectively, and A is the 4×4 Mueller Matrix.

2.4 Derivation of the Mueller Scattering Matrix

The following discussion for the derivation of the Mueller matrix of scattering is taken directly from Bohren and Huffman (1983) for the sake of completeness.

2.4.1 General Formulation

Given a particle of specified size, shape and optical properties that is illuminated by an arbitrarily polarized monochromatic wave, we are interested in determining the electromagnetic field at all points in the particle and at all points of the homogeneous medium in which the particle is embedded.

The field inside the particle is denoted by (E_1, H_1); the field (E_2, H_2) in the medium surrounding the particle is the superposition of the incident field (E_i, H_i) and the scattered field (E_s, H_s) (see Fig.1):

$$\begin{aligned} E_2 &= E_i + E_s, \\ H_2 &= H_i + H_s \end{aligned} \tag{6}$$

where

$$\begin{aligned} E_i &= E_o exp[i(kx - \omega t)], \\ H_i &= H_o exp(ikx - i\omega t) \end{aligned} \tag{7}$$

Here $k = 2\pi/\lambda$ is the wavenumber in the surrounding medium and ω is the angular frequency. The fields must satisfy *Maxwell's* equations

$$\nabla \cdot E = 0, \tag{8}$$

$$\nabla \cdot H = 0, \tag{9}$$

$$\nabla \times E = i\omega\mu H, \tag{10}$$

$$\nabla \times H = -i\omega\varepsilon E, \tag{11}$$

at all points where ε, the dielectric constant and μ, the magnetic permeability are continuous. However, on crossing the boundary between particle and medium, there is a sudden change in ε and μ. Therefore, there is a discontinuity at the boundary. To overcome this difficulty, the following conditions are imposed on the fields:

$$[E_2(x) - E_1(x)] \times \hat{n} = 0, \tag{12}$$

$$[H_2(x) - H_1(x)] \times \hat{n} = 0, \tag{13}$$

Here, x on S, where $\hat{n}$ is the outward directed normal to the surface S of the particle (see Figure 1).

The formulation given here is for scattering of plane monochromatic waves. We use the fact that an arbitrarily polarized wave can be expressed as the superposition of two orthogonal polarization states. Hence, we need to solve each scattering problem twice to determine the scattering of an arbitrarily polarized plane wave. Of course, the spectral nature of light can be accounted for by solving the problem for different wavelengths.

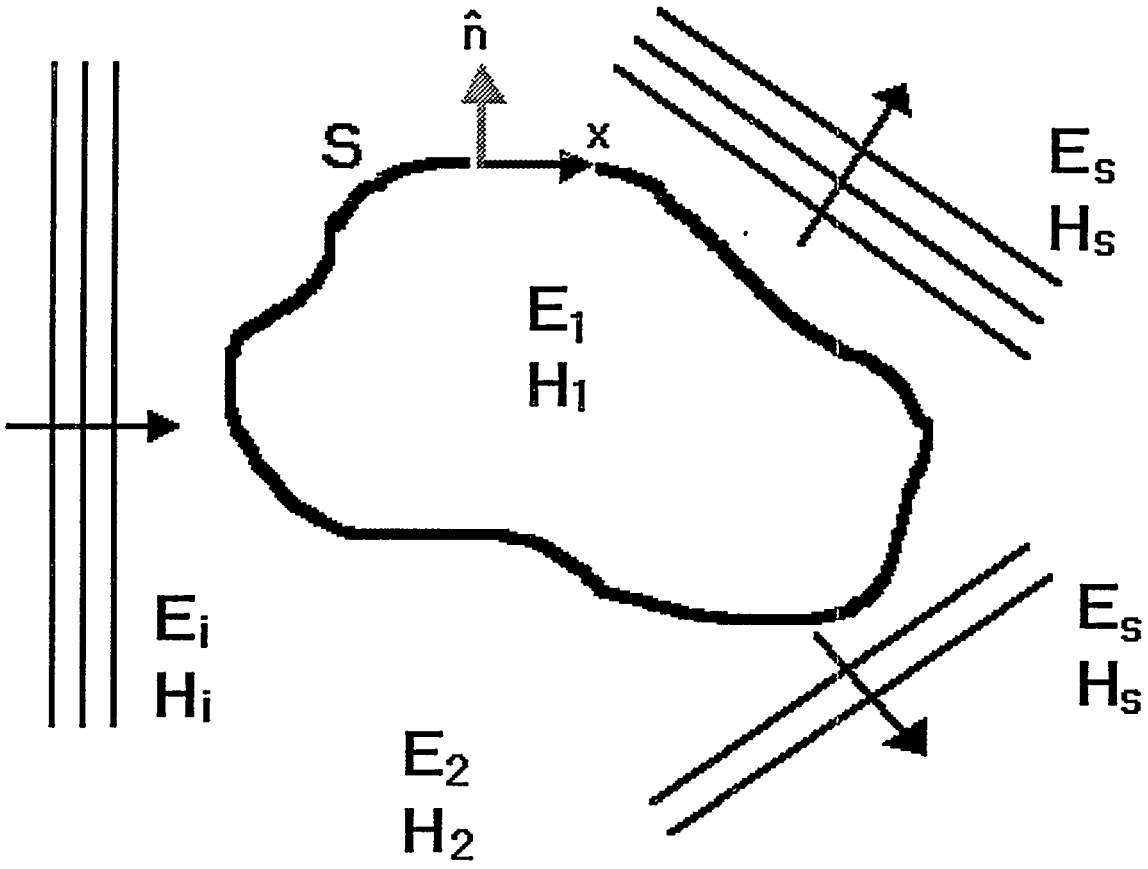

Figure 1: Nomenclature for scattering of EM waves by an arbitrary shaped particle.

2.4.2 The Amplitude Scattering Matrix

Let us consider an arbitrary particle that is illuminated by a plane harmonic wave. A rectangular Cartesian coordinate system, (x, y, z) is chosen with the origin O at A. Orthonormal basis vectors $\hat{e}_x, \hat{e}_y$ and $\hat{e}_z$ are chosen in the directions of the positive x, y and z axes. A scattering plane is defined by the scattering direction $\hat{e}_r$ and the forward direction $\hat{e}_z$ with an azimuthal angle of ϕ from the positive x-axis. The incident electric field E_i in the xy plane is resolved as follows:

$$\begin{aligned} E_i &= (E_{o\|}\hat{e}_{\|i} + E_{o\perp}\hat{e}_{\perp i})exp[i(kz - \omega t)] \\ &= E_{\|i}\hat{e}_{\|i} + E_{\perp i}\hat{e}_{\perp i} \end{aligned} \tag{14}$$

where $k = 2\pi n/\lambda$ is the wave number in the medium surrounding the particle, n is the refractive index, and λ is the wavelength of the incident light.

At sufficiently large distances from the origin ($kr \gg 1$), in the far-field region, the scattered electric field E_s is approximately *transverse* ($\hat{e}_r.E_s \simeq 0$) and has been shown by Jackson (1975) to have the asymptotic form

$$E_s \sim \frac{e^{ikr}}{-ikr}A, \qquad kr \gg 1 \tag{15}$$

where $\hat{e}_r.A = 0$. Hence the scattered field in the far-field region may be written as

$$E_s = E_{\|s}\hat{e}_{\|s} + E_{\perp s}\hat{e}_{\perp s} \tag{16}$$

$$\begin{aligned} \hat{e}_{\|s} &= \hat{e}_\theta, \\ \hat{e}_{\perp s} &= -\hat{e}_\phi, \\ \hat{e}_{\perp s} \times \hat{e}_{\|s} &= \hat{e}_r \end{aligned} \tag{17}$$

Because of the linearity of the boundary conditions, the amplitude of the field scattered by an arbitrary particle is a linear function of the amplitude of the incident field. The relation between incident and scattered fields is conveniently written in matrix form as

$$\begin{Bmatrix} E_{\|s} \\ E_{\perp s} \end{Bmatrix} = \frac{e^{ik(r-z)}}{-ikr} \begin{pmatrix} S_2 & S_3 \\ S_4 & S_1 \end{pmatrix} \begin{Bmatrix} E_{\|i} \\ E_{\perp i} \end{Bmatrix} \tag{18}$$

where the elements $S_j (j = 1, 2, 3, 4)$ constitute the *amplitude scattering matrix* and depend, in general, on the zenith angle θ and the azimuthal angle ϕ.

Each of the four amplitude scattering matrix elements has real and imaginary parts which have to be measured for all values of θ and ϕ. To do so we have to measure the amplitude and phase of the light scattered in all directions for two incident orthogonal polarization states. In general, measurement of the phase of the scattered light is difficult and

few such experiments have been performed. Because of this, the scattering matrix elements are not measured directly. These are related to quantities whose measurement poses fewer experimental problems than phases. These quantities are explored in the following sections.

2.4.3 The Mueller Scattering Matrix

Once the distribution of the electromagnetic fields inside and scattered by the particle are obtained, the time averaged Poynting vector S can be determined at any point in the medium surrounding the particle as

$$\begin{aligned} S &= \frac{1}{2}Re\{E_2 \times H_2^*\} = S_i + S_s + S_{ext} \qquad (19)\\ S_i &= \frac{1}{2}Re\{E_i \times H_i^*\} \\ S_s &= \frac{1}{2}Re\{E_s \times H_s^*\} \\ S_{ext} &= \frac{1}{2}Re\{E_i \times H_s^* + E_s \times H_i^*\} \end{aligned}$$

Here S_i is the Poynting vector associated with the incident wave, S_s is that for the scattered field, and S_{ext} is the term that arises because of the interaction between the incident and scattered waves.

Let us consider a detector placed at a distance r from a particle in the far-field region, with its surface ΔA aligned normal to $\hat{e}_r$. The detector will record a signal proportional to $S_s.\hat{e}_r.\Delta A$. The detector "sees" only the scattered light provided that it does not "look at" the source of incident light. From Eqs. (15) and (19) it follows that

$$\begin{aligned} S_s.\hat{e}_r.\Delta A &= \frac{k}{2\omega\mu}\frac{|A|^2}{k^2}\Delta\Omega \qquad (20)\\ k &= \frac{2\pi}{\lambda} \qquad (21)\\ \omega &= 2\pi\nu \qquad (22) \end{aligned}$$

where $\Delta\Omega = \Delta A/r^2$ is the solid angle subtended by the detector. Thus we obtain $|A|^2$ as a function of the direction by recording the detector response at various locations on a hemisphere surrounding the particle.

By interposing various polarizers between particle and detector and recording the resulting irradiances, we obtain the Stokes parameters of the light scattered by a particle:

$$\begin{aligned} I_s &= < E_{\|s}E_{\|s}^* + E_{\perp s}E_{\perp s}^* > \qquad (23)\\ Q_s &= < E_{\|s}E_{\|s}^* - E_{\perp s}E_{\perp s}^* > \qquad (24)\\ U_s &= < E_{\|s}E_{\perp s}^* + E_{\perp s}E_{\|s}^* > \qquad (25)\\ V_s &= i < E_{\|s}E_{\perp s}^* - E_{\perp s}E_{\|s}^* > \qquad (26) \end{aligned}$$

Here, the multiplicative factor $k/2\omega\mu$ is not written explicitly. The relation between incident and scattered Stokes parameters is obtained from the amplitude scattering matrix Eq. (18) as

$$\begin{Bmatrix} I_s \\ Q_s \\ U_s \\ V_s \end{Bmatrix} = \frac{1}{k^2 r^2} \begin{pmatrix} S_{11} & S_{12} & S_{13} & S_{14} \\ S_{21} & S_{22} & S_{23} & S_{24} \\ S_{31} & S_{32} & S_{33} & S_{34} \\ S_{41} & S_{42} & S_{43} & S_{44} \end{pmatrix} \begin{Bmatrix} I_i \\ Q_i \\ U_i \\ V_i \end{Bmatrix} \tag{27}$$

$$S_{11} = \frac{1}{2}(|S_1|^2 + |S_2|^2 + |S_3|^2 + |S_4|^2) \tag{28}$$

$$S_{12} = \frac{1}{2}(|S_2|^2 - |S_1|^2 + |S_4|^2 - |S_3|^2) \tag{29}$$

$$S_{13} = Re\{S_2 S_3^* + S_1 S_4^*\} \tag{30}$$

$$S_{14} = Im\{S_2 S_3^* - S_1 S_4^*\} \tag{31}$$

$$S_{21} = \frac{1}{2}(|S_2|^2 - |S_1|^2 - |S_4|^2 + |S_3|^2) \tag{32}$$

$$S_{22} = \frac{1}{2}(|S_2|^2 + |S_1|^2 - |S_4|^2 - |S_3|^2) \tag{33}$$

$$S_{23} = Re\{S_2 S_3^* - S_1 S_4^*\} \tag{34}$$

$$S_{24} = Im\{S_2 S_3^* + S_1 S_4^*\} \tag{35}$$

$$S_{31} = Re\{S_2 S_4^* + S_1 S_3^*\} \tag{36}$$

$$S_{32} = Re\{S_2 S_4^* - S_1 S_3^*\} \tag{37}$$

$$S_{33} = Re\{S_1 S_2^* + S_3 S_4^*\} \tag{38}$$

$$S_{34} = Im\{S_2 S_1^* + S_4 S_3^*\} \tag{39}$$

$$S_{41} = Im\{S_2^* S_4 + S_3^* S1\} \tag{40}$$

$$S_{42} = Im\{S_2^* S_4 - S_3^* S1\} \tag{41}$$

$$S_{43} = Im\{S_1 S_2^* - S_3 S_4^*\} \tag{42}$$

$$S_{44} = Re\{S_1 S_2^* - S_3 S_4^*\} \tag{43}$$

The 4×4 matrix in Equation 27 is the *Scattering Matrix* or the *Mueller Matrix* for scattering by a single particle. Note that not all the 16 elements of the scattering matrix are independent. Only seven of them are independent corresponding to the four moduli $|S_j|$ $(j = 1,2,3,4)$ and the three differences in phase between the S_j. Thus, there must be nine independent relations among the S_{ij}; these are given by Abhyankar and Fymat (1969).

If unpolarized light of irradiance I_i is incident on one or more particles, the Stokes parameters of the scattered light are

$$\frac{I_s}{I_i} = S_{11}, \qquad \frac{Q_s}{I_i} = S_{21}, \qquad \frac{U_s}{I_i} = S_{31}, \qquad \frac{V_s}{I_i} = S_{41} \tag{44}$$

Therefore S_{11} specifies the angular distribution of the scattered light given unpolarized incident light. The degree of polarization of the scattered light is given by

$$\sqrt{(S_{21}^2 + S_{31}^2 + S_{41}^2)/S_{11}^2} \tag{45}$$

The Stokes parameters of the light scattered by a collection of randomly oriented particles are the sum of the Stokes parameters of the light scattered by the individual particles. Therefore, the scattering matrix for such a collection is merely the sum of the individual particle scattering matrices. In general, there are 16 non-zero Mueller matrix elements.

2.5 Symmetry in Mueller matrices for scattering in an arbitrary direction

A cloud, or medium, of scattering particles contains many identical particles with different orientations in space. In this section we will discuss the simplifications of the scattering matrix that will result if we make certain assumptions about the distribution of orientations.

If the scattering matrix of a particle in a particular position and for a particular direction is known, the scattering matrix of the same particle, or its mirror image, in certain symmetrical positions is also known. When different particles or differently oriented particles are present together in the same medium, the elements of the individual scattering matrices have to be added to obtain the scattering matrix of the medium. The addition causes certain non-diagonal elements of the final matrix to vanish and others to become equal, depending on the exact assumptions made.

Let us consider a direction for which the scattering angle is not 0° or 180°. The directions of incidence and scattering define the *scattering plane.* This is taken as the plane of reference. The line in the scattering plane that bisects the angle between the incident and scattered beam is called the *bisectrix.* The plane through the bisectrix and perpendicular to the plane of scattering is called the *bisectrix plane.*

A given position of the particle is taken as the initial position (a). Three other positions for which the scattering matrix may be expressed in terms of the same coefficients as in position (a). Rotation of 180° about the bisectrix plane puts the particle (a) in the position (b). (b) is called the *reciprocal position* of (a). Mirroring with respect to the plane of scattering gives a position (c). Mirroring with respect to the bisectrix plane gives another position (d). The corresponding amplitude matrices are given as (Van de Hulst, 1957)

$$\overset{(a)}{\begin{pmatrix} S_2 & S_3 \\ S_4 & S_1 \end{pmatrix}} \overset{(b)}{\begin{pmatrix} S_2 & -S_4 \\ -S_3 & S_1 \end{pmatrix}} \overset{(c)}{\begin{pmatrix} S_2 & -S_3 \\ -S_4 & S_1 \end{pmatrix}} \overset{(d)}{\begin{pmatrix} S_2 & S_4 \\ S_3 & S_1 \end{pmatrix}} \tag{46}$$

We shall now make certain assumptions about the distribution of particles among these positions:

1. The cloud contains one kind of particles. For each particle in one position a particle in the reciprocal position is found. Adding the scattering matrices of (a) and (b) we get the following matrix

$$\begin{pmatrix} S_{11} & S_{12} & S_{13} & S_{14} \\ S_{12} & S_{22} & S_{23} & S_{24} \\ -S_{13} & -S_{23} & S_{33} & S_{34} \\ S_{14} & S_{24} & -S_{34} & S_{44} \end{pmatrix} \qquad 10 \textit{ parameters} \tag{47}$$

2. The cloud contains particles and their corresponding mirror image particles with respect to the plane of scattering. For any particle in position (a) a mirror particle in position (c) is found. In this case the resulting matrix is

$$\begin{pmatrix} S_{11} & S_{12} & 0 & 0 \\ S_{12} & S_{22} & 0 & 0 \\ 0 & 0 & S_{33} & S_{34} \\ 0 & 0 & S_{43} & S_{44} \end{pmatrix} \qquad 8 \textit{ parameters} \tag{48}$$

3. The cloud contains particles and their mirror image particles with respect to the bisectrix plane. For any particle in position (a) a mirror particle in position (d) is found. In this case the resulting matrix is

$$\begin{pmatrix} S_{11} & S_{12} & S_{13} & S_{14} \\ S_{12} & S_{22} & S_{23} & S_{24} \\ S_{13} & S_{23} & S_{33} & S_{34} \\ -S_{14} & -S_{24} & -S_{34} & S_{44} \end{pmatrix} \qquad 10 \textit{ parameters} \tag{49}$$

4. The cloud contains particles and their mirror particles, while any two of the preceding assumptions are made. The third one follows automatically so that there are equal numbers of particles in positions (a), (b), (c), and (d). The resulting matrix has the form

$$\begin{pmatrix} S_{11} & S_{12} & 0 & 0 \\ S_{12} & S_{22} & 0 & 0 \\ 0 & 0 & S_{33} & S_{34} \\ 0 & 0 & -S_{34} & S_{44} \end{pmatrix} \qquad 6 \textit{ parameters} \tag{50}$$

5. The cloud contains one kind of asymmetric particles with random orientation. The assumptions of Case 1 are then fulfilled and the scattering matrix has 10 parameters.

6. The cloud contains particles that have a plane of symmetry and are randomly oriented. In this case the assumptions of Case 4 are satisfied and the scattering matrix has 6 parameters.

2.6 Symmetry in Mueller Matrices for Particles in Flames

Flames contain a large number of soot particles. These particles are randomly oriented and it may be possible to find a plane of symmetry for them. Hence the assumptions of Case 6 in the previous section are fulfilled and the Mueller matrix in this case consists of six independent parameters.

2.7 Soot Agglomerates

Individual soot particles are spherical in shape with diameters of about 20 nm to 40 nm. The properties of these individual soot particles can easily be calculated from theory provided that the complex index of refraction and number density data are available. Unfortunately, at many times soot is present in agglomerated form, which changes during the combustion process. The soot particles will be modeled as either small spheres or agglomerates, employing the Rayleigh or discrete dipole approximations, respectively. The latter approximation (DDA; cf. Draine, 1988, or Mengüç, et al., 1992) is computationally quite involved; however, the volume fraction distribution of soot particles as measured from experimental studies should be determined using such a rigorous formulation. Otherwise, the effect of local turbulent fluctuations on soot radiation cannot be quantified. Rayleigh approximation will be used only if there is lack of information or evidence of agglomeration.

Recently, Manickavasagam and Mengüç (1994) have completed a new algorithm, AGGLOME, based on the volume integral formulation of the electromagnetic wave propagation. With this algorithm, it is possible to model much larger and fractal-like soot agglomerates as shown in Figure 2. These numerical techniques would yield correct β_λ, κ_λ, and σ_λ coefficients *only* if the volume fraction of particles is known with great accuracy.

Figure 3 depicts the scattering phase function for coal/soot clouds as a function of soot volume loading. It is assumed that coal has a size distribution with mean diameter of 2.5 μm, and soot is considered in agglomerated form. The results indicate that the volume fraction of soot can be determined if the experiments are carried out to measure the scattering intensity from 30-130 degrees. More detailed numerical comparisons are given in a paper by Manickavasagam and Mengüç, which is currently being prepared. We will submit it to DOE after it is completed.

3 EXPERIMENTAL SYSTEMS

3.1 Introduction

The laboratory facility for light scattering measurements for particulate diagnostics in coal flames has been almost completed. In spite of extensive problems related to both laser and

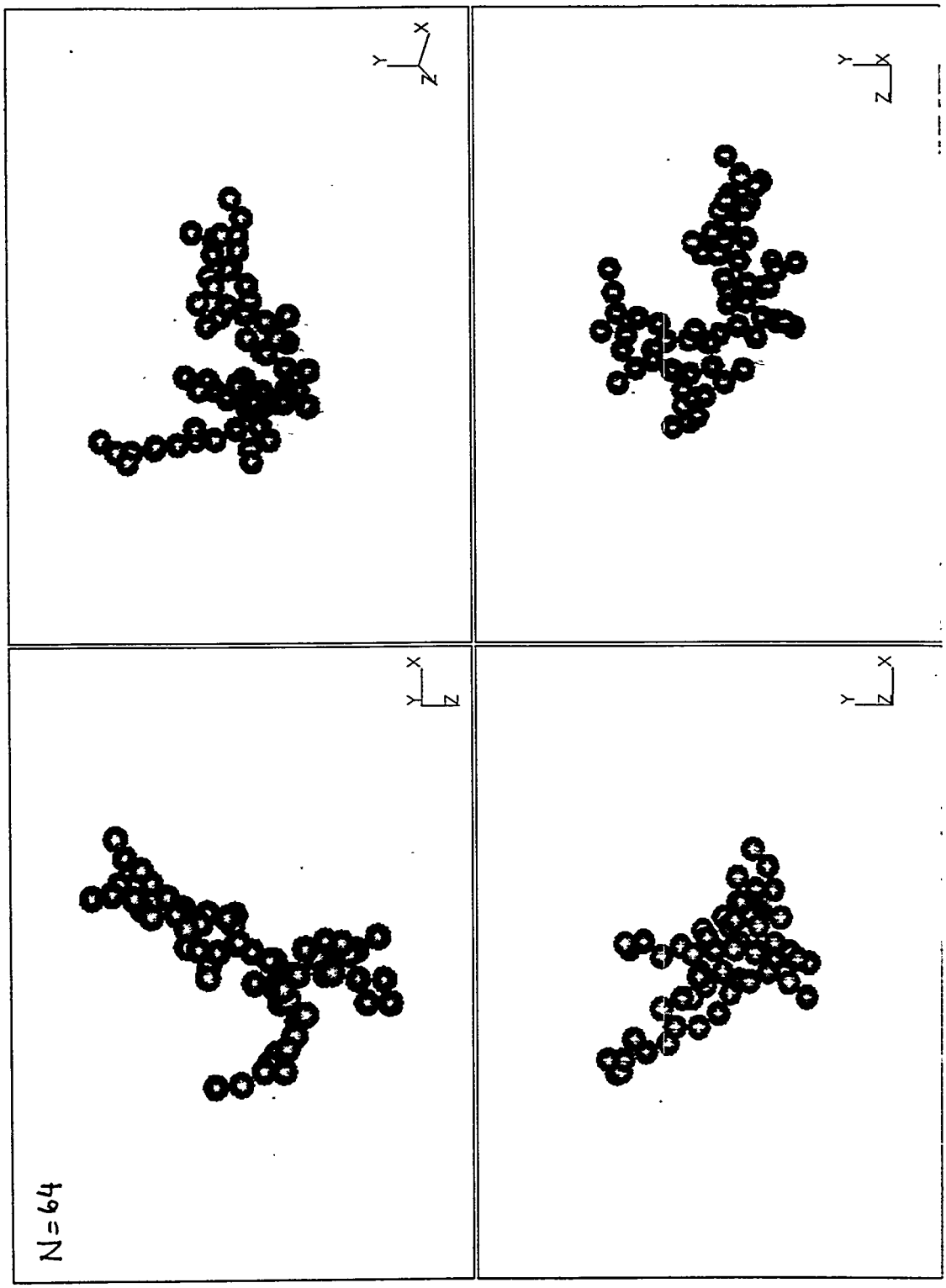

Figure 2: Typical structure of fractal-like soot agglomerates modeled using the AGGLOME algorithm.

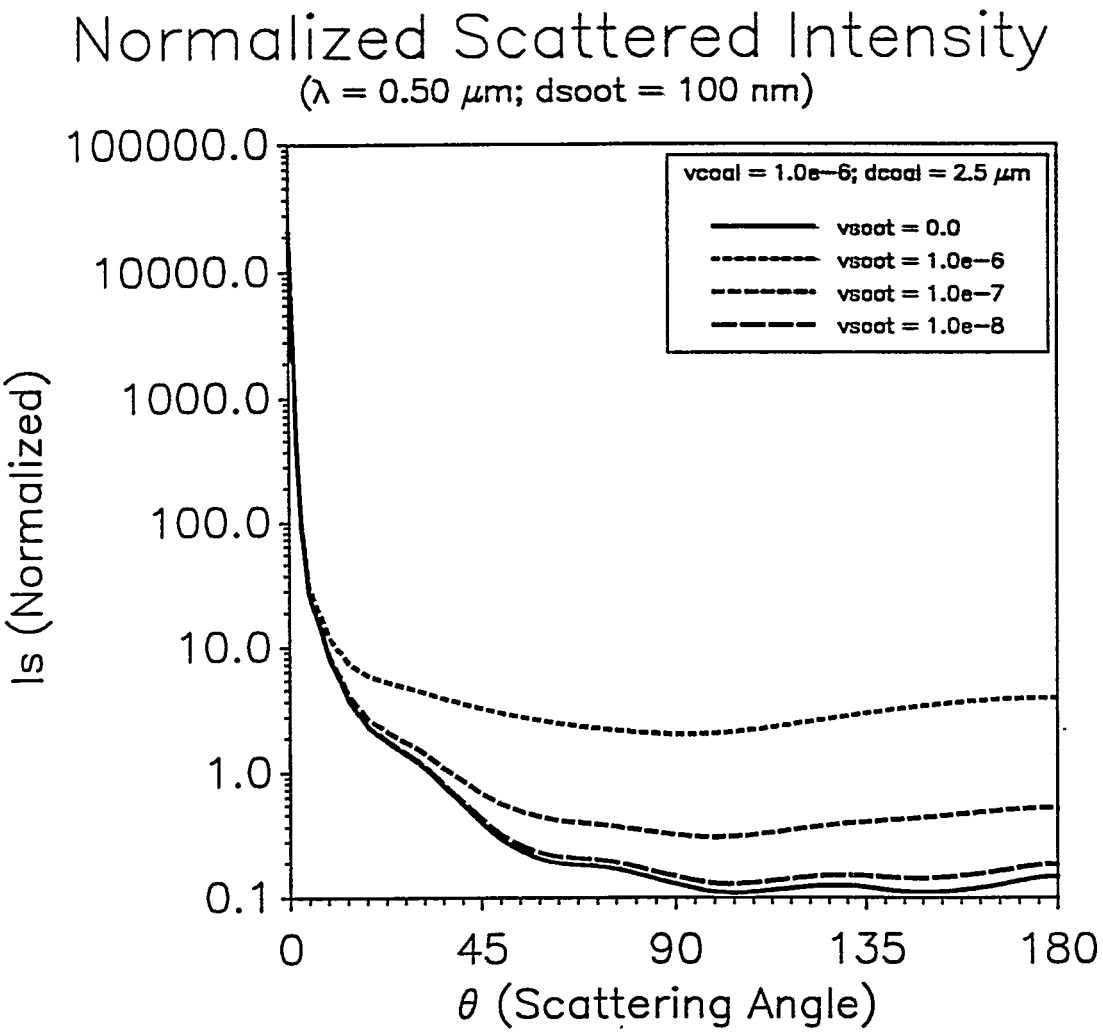

Figure 3: Scattering phase function of a coal-soot cloud as a function of soot loading.

laboratory setting, a fully functional diagnostic system based on a Nd:YAG laser (4 wavelengths), a Raman shifter (additional four wavelengths) and a CO_2-laser (Far-infrared wavelength at λ=10.6μm has been completed and now operational. An axisymmetric co-flow burner for generating diffusion flames of varying stoichiometry is used to sustain combustion of the pulverized coal, fed with the oxidizer as a slurry from a fluidized bed.

The highlight of the last year's experimental achievement is the development of a diagnostic system based on a high power, short pulse, solid state Nd:YAG laser, which will be used to make scattering measurements at wavelengths and scattering angles that have hitherto not been possible. Figure 4 depicts the lay-out of the Nd:YAG laser experimental system.

The details of the various components of the experimental apparatus (including the laser, the detectors, and the data acquisition system), and the process of making the set-up functional are discussed below. There is detailed guideline to some aspects of operating this facility, e.g., a user's manual written for the YAG laser to complement the manufacturer's manual, and to facilitate proper operation of the instrument. The design and construction of the YAG laser diagnostics system was performed mainly by Dr. Ghosal. Dr. Manickavasagam and Mr. Govindan also helped Dr. Ghosal during his efforts.

3.2 Nd:YAG Laser

The Nd:YAG laser is now in operation emitting light at a fundamental wavelength of 1064 nm, and through frequency-doubling, in the green at 532 nm. Other crystals have been acquired for further frequency conversion to generate light at 266 nm and 355 nm. While the rated energy per pulse is 400 mJ and 150 mJ for the fundamental and the first harmonic outputs, respectively, we are currently achieving much better non-linear frequency conversion efficiency (240 mJ per pulse at the first harmonic of 532 nm).

This Q-switched laser produce pulsed radiation at 30 Hz with a very short pulse width of 4 to 9 ns, resulting in a very high instantaneous power output of tens of gigawatts. The Gaussian beam diameter of about 6 mm. This high peak intensity produces better signal/noise (S/N) ratio for scattered light measurements than that possible with longer pulse-width lasers, particularly at angles where the scattered intensity is low. Additionally, the use of pulsed light source allows discrimination of scattered light from emitted light.

3.2.1 Laser Intensity Modulation

Depending on the type of the experiments to be performed, the laser intensity requires some adjustment. For this purpose, however, neutral density filters cannot be used directly in the beam path (even silica or quartz filters) because the high peak power causes them to shatter instantly. We used two neutral-density filters successively only to reduce the

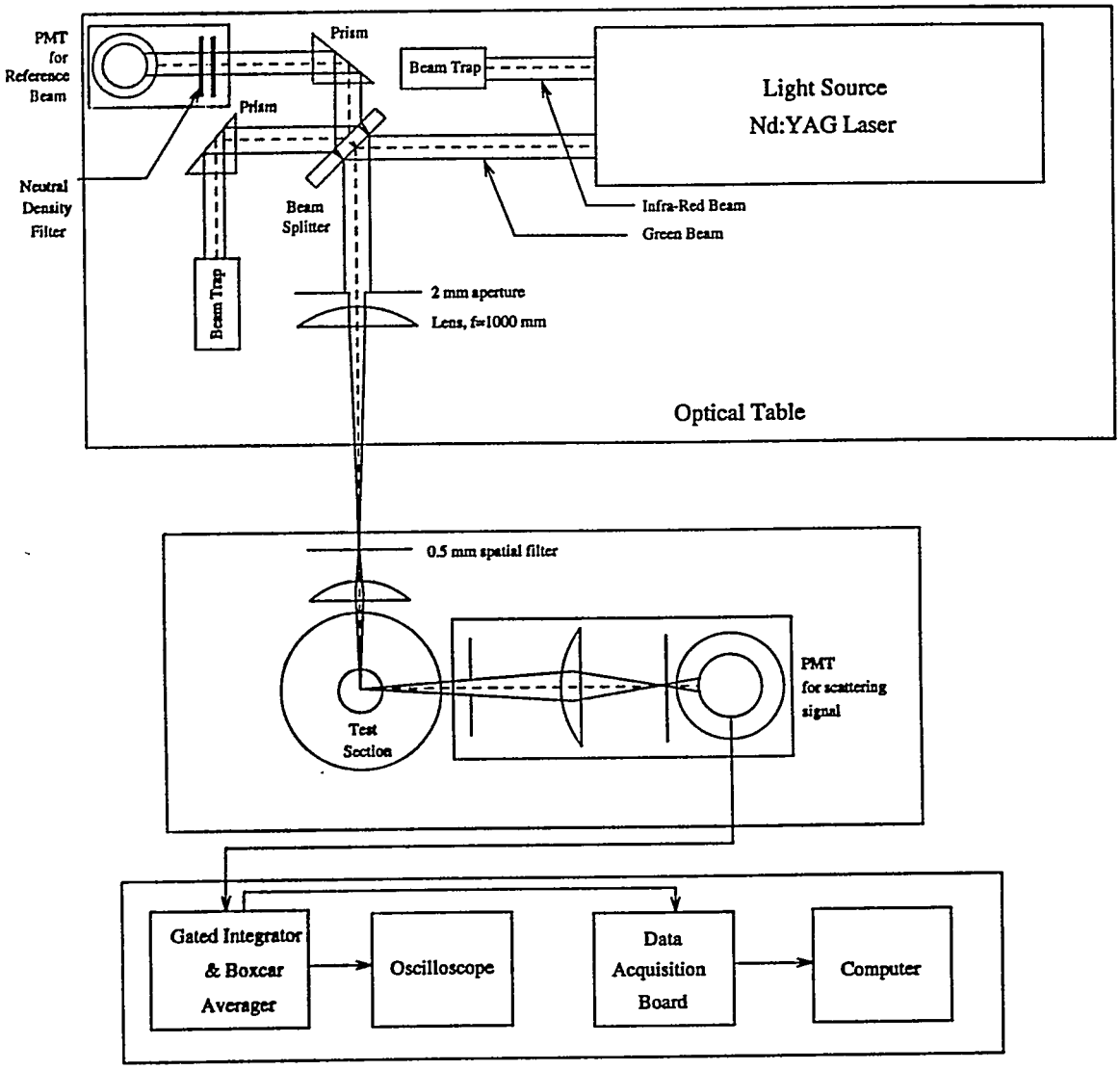

Figure 4: Schematic of the Nd:YAG laser nephelometer.

intensity of laser light *reflected* by intermediate optics (used as a reference signal to monitor the pulse-to-pulse intensity) by an overall factor of 10^{-7}.

An alternative method for controlling laser intensity is to modulate the pump flashlamp intensity. While this method is not recommended by the laser manufacturers[1], it appears to be common practice in many laboratories. Additionally, this is not a precise method since the inverted Nd^{3+} population may change for the same lamp intensity setting each time the laser is turned on.

The laser manufacturer recommends intensity modulation by use of the Q-Switch Synch timing adjust circuit which can change the Q-switch firing time with respect to the flashlamp pumping. However, greater the Q-Switch mis-timing (and lower the output intensity), the greater is the 'jitter' in the signal (i.e., the laser pulse fluctuates randomly by several nanoseconds about its mean position). Hence this technique does not seem to be acceptable for controlling beam intensity when making measurements, although it is convenient for aligning optics.

The safest and most convenient way to adjust beam intensity is to use an external polarizer. However, they are expensive, and wavelength dependent. Mainly because we are planning to expand this system to a multi-wavelength tool, this alternative was not found acceptable.

One of the easiest approaches is the use of a succession of beam splitters (or windows). Although the reduction in intensity will not be continuously variable, still this approach is preferable to the others. The main drawback of this method is the large number of reflections one need to control. Currently, we are experimenting with this idea.

3.2.2 Laser Equipment Problems

Two main problems cost us more than two months of experimental research time during the last twelve months. Within a month of operation, the laser Q-switch failed unexpectedly. On examination, it was found that a portion of the refracted index-matching fluid in the Pockels Cell had somehow drained away, This loss of fluid resulted in increased reflection between the windows, which in turn damaged the windows. No obvious explanation was available, and the damage was ascribed to sample failure. The Q-switch was 'rebuilt' by the manufacturer (Cleveland Crystals) and delivered to our laboratory after a month.

Both the laser flashlamps effectively 'burnt out' within a week of each other after a couple of months of occasional use of the laser, well ahead of the rated lifetime. The probable reason is that the lamps have a fixed shelf-life, irrespective of their frequency of use.

A Laser User's Guide has been written to complement the information in the manual

[1]Apparently lower lamp energy causes the laser beam to diverge inside the cavity.

supplied by Quanta-Ray for their GCR 150-30-189 Pulsed Nd:YAG laser. This more readable guide contains step-by-step instruction for operating the laser, useful practical tips, as well as comprehensive instructions for its maintenance.

3.3 Detectors

For measurements using the available lasers, three sets of detectors are needed: one for the visible, one for the near infrared (1064 nm), and one for the CO_2 laser (at 10.6 μm).

For measurement at visible wavelengths, photomultiplier tubes (PMT) are being used because of their excellent responsitivities. Two nine-stage, side-on PMTs (a Burle 4840 and a Hamamatsu R446), with a detection range of 200–900 nm, measure the scattered light and the reference signal simultaneously. A stable high voltage power supply is being purchased for use with the PMTs. Suitable mounts and housings for the PMTs have been fabricated to minimize detection of stray light.

For measurement in the near infrared, high-speed germanium photodiodes (Hamamatsu model B2297, rise-time = $\sim$2 ns) are being used. They are rugged, and have the added advantage that they can be operated using low-voltage DC cells. They have been tested using the 532 nm light from the YAG laser for their saturation behavior.

For the CO_2 laser, the detectors used are pyroelectric type (Hamamatsu, Model P2613-03) with a high impedance single crystal made of $LiTaO_3$. Incident light causes a temperature change in the $LiTaO_3$ crystal, which in turn generates electric charge on the crystal surface. These detectors have a spectral range of 8–15 μm. The sensitivity of the detectors is greatest close to a pulse frequency of 1 Hz and decreases exponentially with increasing frequency. The detectors are connected to a transistor socket located within a specially designed detector mount. A power supply is used to input 10 volts d.c. into each detector.

3.4 Gated-Integrator/Boxcar Averager

The SRS 250 gated-integrator and boxcar averager module is a versatile, high speed instrument for recovering fast, low duty cycle, analog signal from relatively noisy backgrounds. The gate generator, which can be triggered externally (e.g., by the laser's Q-switch Synch output signal), provides an adjustable delay in the range of 1 ns–10 ms, and generates a gate of continuously variable width in the range 2 ns–15 μs. Only that part of the signal overlapping with the gate is recorded. A dual-channel 400 MHz oscilloscope (HP 54502A) is used to adjust the delay so that the gate is positioned over the signal.

The fast-gated integrator integrates the input signal, its output being normalized by the gate width to produce a (further amplifiable) voltage proportional to the average input signal during the sampling gate. To improve the S/N by a maximum factor of hundred, the output can be averaged over 1–10,000 samples thus reducing the contribution of the

random white noise. To remove baseline drift or background noise from the signal, one can use SR250's Active Baseline Subtraction circuitry. In this method, the sampling is performed at twice the signal frequency, the sample with no signal present being inverted and added to the moving average.

The averaged signal can be monitored using analog or digital meters on the SRS 280 System Mainframe. The Computer Interface Module (SRS 245) is used to transfer the data to a PC where a commercial data acquisition software (LabTech) receives, plots, and records the data. Two gated integrators are being used to acquire both the scattered signal and the reference signal simultaneously.

In scattering experiments, we are using both the active and passive noise reduction methods described above, and averaging over $\geq$30 samples. In order to eliminate signal fluctuations due to laser 'jitter', it's advisable to use a gate of sufficient width so that it spans the entire signal (about 50 ns). However, the detector wiring must have proper impedance matching so that there is little 'ringing' following the signal and within the gate.

3.5 Optical Components

Because anti-reflection coated on our high power laser lenses and prisms are very wavelength specific (each set barely covers a range of 100–200 nm), we decided to use uncoated components. Whenever possible, we have used fused silica components which are less expensive than quartz components, and tolerate high laser power for sufficiently long time periods. Prisms have been used to construct beam steering mechanisms for directing the laser beam into the flame. Fused silica plano-convex lens is used for focusing the laser beam. Several beam traps have been constructed to trap the ubiquitous reflections off intermediate components.

A schematic of the current optical arrangement is shown in Figure 4. The laser light is steered at right angles using a fused-silica prism, followed by another beam steering combination consisting of two prisms (not shown here) which raises the beam (perpendicular to the plane of the page) so that the latter reaches the level of the burner, following the train of lenses. All the above optical components, including the laser, are mounted on an optical table. The detector (PMT or infrared detector), lens, and the aperture are housed in an black aluminum box for shielding against stray scattered laser light. The box, in turn, is mounted on a platform that can rotate around the burner, thus making possible angular scattering measurements in the range 13° to 155°, measured from the forward direction.

The experimental set-up is now ready for measurements, except for a modulator for the laser intensity, on which we will shortly make a decision.

3.6 Burner

A coflow diffusion flame burner has been built for all studies related to coal, soot, and ash radiative properties at elevated temperatures. The overall height of the burner assembly is 35 cm. It is mounted on a mechanism enabling vertical and horizontal translations of about 15 and 5 cm, respectively. The burner consists of a central fuel tube surrounded by a co-annular oxidizer tube having diameters of 1 and 5 cm, and has been designed to obtain a flat velocity profile of the oxidizer and the fuel.

The oxidizer tube has two diametrically opposite inlet ports which make possible an even distribution of the oxidizer across the cross-section of the tube. An 8 cm deep layer of 4 mm diameter glass beads within the conical portion of the oxidizer passage and four thin metallic sheets having (uniformly distributed) 3 mm diameter holes placed at constant intervals across the cylindrical portion of the oxidizer passage ensure a stable and radially-uniform flow of the oxidizer. Coal-air mixture is fed into the central fuel tube at the bottom of the burner, which is mixed with ethylene to produce a premixed flame.

Gas flow into the central fuel tube and the outside oxidizer (air) tube are monitored using Matheson 601 and 605 series flow-meters, respectively. Higher flow rates of oxidizer, which under certain situations may be necessary to stabilize the flame, are monitored by using two 605 flow-meters connected in parallel. Calibration of the 605 flow-meters is accomplished with a wet test meter (Precision Scientific Company, Catalog No. 63115) and the calibration of the 601 flow-meter is accomplished by recording the velocity of a soap bubble in a glass tube of known diameter. Ethylene (99.5% purity, Central Welding Supplies) was used as fuel. Line air supply to the laboratory, filtered and precisely regulated, is used as oxidizer.

3.7 Fluidized Bed for Flame Experiments

A fluidized bed made of Plexiglas has been fabricated for feeding coal to the burner. It is 44.5 cm high and has a diameter of 11.4 cm. The two ends of the bed are sealed to prevent any leakage of coal or air carried into the burner. At the bottom end, the sealing cork supports two tubes (of external diameters 6 mm and 4 mm, and internal diameters 4 mm and 3 mm, respectively) to supply air to fluidize coal particles in the bed. The smaller tube (which enters the bottom of the fluidized bed) terminates as a helically coiled tube inside the bed and helps in circulating the air inside. The air from the larger tube at the bottom gives a forward momentum to the coal particles inside the bed. Because of this momentum gain, the coal particles come out of the bed through the tube (external diameter 10 mm and internal diameter 6 mm) attached to the cork at the top of fluidized bed.

The coal-air mixture issuing out of the bed is discharged into the center tube of the burner, where it is mixed with ethylene and is ignited at the tip of the burner. The flow rate of coal can be controlled by adjusting the flow rate of air which enters the bed. With

this set up flow rates as low as 0.1 gm/min can be achieved. Since it was found that a higher flow rate of coal resulted in lift-off of the flame, flow rates in the present study are restricted to 0.3 to 0.6 gm/min. The coal flow rate was measured by collecting coal particles coming out of the fluidized bed for 1 minute, and weighing them on a chemical balance.

4 FUTURE WORK

We expect to complete this work within the next six months. All the important parts of both the theoretical and the experimental work is complete. We are currently in the phase of fine tuning the experimental system and computer algorithms. The details of the results will be outlined in the final report to the DOE.

5 REFERENCES

[1] Abhyankar, K.D., Fymat, A.L., (1969), "Relations between the elements of the phase matrix for scattering", *Journal of Mathematical Physics*, Vol. 10, No. 10, pp. 1935-1938.

[2] Beardsley Jr., G.F., (1968), "Mueller scattering matrix of sea water", *Journal of the Optical Society of America*, Vol. 58, No. 1, pp. 52-57.

[3] Bohren, C.F., Huffman, D.R., (1983), *Absorption and scattering of light by small particles*, John Wiley, New York.

[4] Boyer, G.R., Lamouroux, B.F., Prade, B.S., (1979), "Automatic measurement of the Stokes vector of light", *Applied Optics*, Vol. 18, No. 8, pp. 1217-1219.

[5] Draine, B.T., (1988), *Astrophysical Journal*, Vol. 333, pp. 848-872.

[6] Fry, E.S., Kattawar, G.W., (1981), "Relationships between elements of the Stokes matrix", *Applied Optics*, Vol. 20, No. 16, pp. 2811-2814.

[7] Ghosal, S., Manickavasagam, S., and Mengüç, M.P., (1994), "Light Scattering Experiments for Simultaneous Determination of Soot and Char Volume Fractions in Coal-Fired Flames", Poster Presentation at the 25th International Symposium on Combustion, Irvine, CA, August 1994.

[8] Holland, A.C., Gagne, G., (1970), "The scattering of polarized light by polydisperse systems of irregular particles", *Applied Optics*, Vol. 9, No. 5, pp. 1113-1121.

[9] Hovenier, J.W., van de Hulst, H.C., van der Mee, C.V.M., (1986), "Conditions for the elements of the scattering matrix", *Astronomy and Astrophysics*, Vol. 157, pp. 301-310.

[10] Hunt, A.J., Huffman, D.R., (1973), "A new polarization-modulated light scattering instrument", *Review of Scientific Instrumentation*, Vol. 44, No. 12, pp. 1753-1762.

[11] Ivezic, A., and Mengüç, M.P., (1994), "An Investigation of Dependent-Independent Scattering Regimes for Soot Particles Using the Discrete Dipole Approximation", submitted to the *International Journal of Heat and Mass Transfer*, 1994.

[12] Kemp, J.C., (1969), "Piezo-optical birefringence modulators: new use for a long-known effect", *Journal of the Optical Society of America*, Vol. 59, No. 8, pp. 950-954.

[13] Kuik, F., Stammes, P., Hovenier, J.W., (1991), "Experimental determination of scattering matrices of water droplets and quartz particles", *Applied Optics*, Vol. 30, No. 33, pp. 4872-4881.

[14] Manickavasagam, S., and Mengüç, M.P. (1994), "Mueller Matrix Components of Fractal-Like Soot Agglomerates", to be submitted to *Applied Optics*.

[15] Mengüç, M.P., Mahadeviah, A., Saito, K., and Manickavasagam, S., (1992), presented at the ASME National Heat Transfer Conference, San Diego, CA, July 1992.

[16] Pritchard, B.S., Elliott, W.G., (1960), "Two instruments for atmospheric optics measurements", *Journal of the Optical Society of America*, Vol. 50, No. 3, pp. 191-202.

[17] van de Hulst, H.C., (1957), *Light scattering by small particles*, Dover Publications, New York.

[18] Thompson, R.C., Bottiger, J.C., Fry, E.S., (1980), "Measurement of polarized light interactions via the Mueller matrix", *Applied Optics*, Vol. 19, No. 8, pp. 1323-1332.